Pharmaceutical Sciences 2026;32(4):611-622
doi:10.34172/ps.43665
https://ps.tbzmed.ac.ir

Original Article

Biodisposition of the Promising JNK Inhibitor IQ-1 and its Metabolite in Rats Following Single Oral Administration

Galina A. Frelikh[1*], Elena A. Yanovskaya[1,2], Alexander P. Lakeev[1,2], Galina A. Chernysheva[1], Vera I. Smolyakova[1], Andrei I. Khlebnikov[3]

[1]Goldberg Research Institute of Pharmacology and Regenerative Medicine, Tomsk National Research Medical Center, Russian Academy of Sciences, 3, Lenin Ave., Tomsk, 634028, Russia
[2]National Research Tomsk State University, 36, Lenin Ave., Tomsk, 634050, Russia
[3]National Research Tomsk Polytechnic University, 30, Lenin Ave., Tomsk, 634050, Russia

ARTICLE INFO

Article History:
Received: December 23, 2025
Revised: June 5, 2026
Accepted: June 8, 2026
ePublished: July 29, 2026

Keywords:
IQ-1, LC-MS/MS, Biodisposition, Pharmacokinetics, Absorption, JNK Inhibitor

Abstract

Introduction: The JNK inhibitor 11*H*-indeno[1,2-*b*]quinoxalin-11-one oxime (IQ-1) and its sodium salt exhibit antioxidant, hemorheological, endothelium-protective, anti-inflammatory, neuroprotective, and cardioprotective properties; however, no published reports describe their tissue distribution. We investigated the biodisposition of IQ-1 and its major metabolite, 11*H*-indeno[1,2-*b*]quinoxalin-11-one (IQ-18), in Wistar rats after a single oral 50 mg/kg dose of IQ-1.

Methods: Male adult Wistar rats (230–260 g) received IQ-1 orally (50 mg/kg). To investigate plasma pharmacokinetics and tissue distribution of IQ-1 and its metabolite IQ-18 in rats, arterial blood was collected from the carotid artery, and tissue samples (liver, kidney, heart, brain, lung, spleen, skeletal muscle, adipose tissue, and duodenum) were harvested following oral administration of 50 mg/kg IQ-1. Mesenteric lymph, bile, and blood from the portal vein and inferior vena cava were also obtained post-dose to clarify the absorption routes and metabolic sites of IQ-1. Chromatographic separation was carried out on an EC Nucleodur C8 ec LC column (150×4.6 mm, 5 µm; Macherey-Nagel, Germany). IQ-1 and IQ-18 were quantified by validated LC-MS/MS method using a LC-20 Prominence system (Shimadzu) and a mass spectrometer 3200 QTRAP (AB Sciex). Analyst 1.6 and MultiQuant 2.1 (AB Sciex) handled data acquisition and analysis. Non-compartmental pharmacokinetic parameters were calculated with WinNonlin 5.2 (Pharsight). Statistics (Mann–Whitney U test; $P<0.05$) were performed in Statistica 12.

Results: The plasma pharmacokinetic parameters for IQ-1 were as follows: C_{max}, 59.69 ng/mL; T_{max}, 1 h; and $T_{1/2}$, 5.58 h. IQ-1 was metabolized to IQ-18, which reached a plasma C_{max} of 2464.06 ng/mL at 8 h. Both compounds were widely distributed in tissues, with the highest tissue-to-plasma ratio observed in the liver. The T_{max} values were 0.5–1 h for IQ-1 and 4–8 h for IQ-18. These data may indicate predominant absorption via the portal vein, extensive hepatic metabolism, and a substantial reduction in the concentrations of both compounds in venous blood following hepatic passage.

Conclusion: Our results provide valuable insights into the pharmacokinetic profile of IQ-1, which may inform future clinical trials.

Introduction

The pharmacokinetic profile of a drug candidate is vital for understanding in vivo interactions with the human body, as it determines the efficacy and toxicity of the compound.[1] Absorption and metabolism are major factors that influence oral bioavailability. Therefore, comprehensive preclinical pharmacokinetic (PK) studies are essential to ensure the success of a drug candidate in clinical trials.[1] These preclinical PK studies, conducted in the early phases of drug development, aim to predict human pharmacokinetics, establish an appropriate dosage regimen, and facilitate the interpretation of efficacy data.[2] Moreover, the pharmacokinetic properties of a drug candidate, along with preliminary results from its safety and efficacy studies, are critical for making the decision to continue or terminate development of a new drug.[3]

Therapeutic strategies are frequently based on the principle of inhibiting signaling pathways implicated in disease pathogenesis. Among these targets, the c-Jun N-terminal kinase (JNK) family is a subject of intense research. As members of the mitogen-activated protein kinase (MAPK) family, JNKs regulate critical cellular processes such as proliferation, differentiation, survival, and cell death responses. Moreover, they play essential roles in diverse physiological functions, including neuronal signaling, immune regulation, embryonic development,

***Corresponding Author:** Galina Frelikh, Email: galina_stykon@mail.ru

© 2026 The Author(s). This is an open access article and applies the Creative Commons Attribution Non-Commercial License (http://creativecommons.org/licenses/by-nc/4.0/). Non-commercial uses of the work are permitted, provided the original work is properly cited.

and metabolic homeostasis.[4] Dysregulated JNK signaling is involved in a wide spectrum of pathologies, such as apoptosis-related disorders, inflammatory diseases, as well as myocardial and cerebral ischemia-reperfusion injury.[5] Furthermore, JNKs contribute significantly to the development of insulin resistance and motor neuron diseases, and are implicated in dysregulated cellular proliferation, tumorigenesis, and neurodegenerative disorders.[4,6,7] Consequently, JNK inhibition represents a promising therapeutic strategy, driving considerable efforts to discover and develop effective, specific, and non-toxic JNK inhibitors.[5-7]

One such specific JNK inhibitor, which is the subject of our research, is 11*H*-indeno[1,2-*b*]quinoxalin-11-one oxime (IQ-1, Figure 1). This compound exhibits high affinity for JNK3 compared to JNK1 and JNK2.[8] The mechanism of action and pharmacological properties of IQ-1 have been extensively investigated in recent years.[9-13] Its sodium salt has demonstrated significant neuroprotective effects in various murine and rat models of ischemia-reperfusion injury.[9,14] Beyond JNK inhibition, IQ-1 releases nitric oxide (NO) during enzymatic metabolism by liver microsomes, which contributes to improved outcomes in models of ischemic stroke and myocardial infarction.[9,10] Studies in animal models and cell cultures have further revealed its antioxidant, hemorheological, endothelium-protective, anti-inflammatory, and antihypertensive properties, underscoring its therapeutic potential for conditions such as rheumatoid arthritis.[8,11-14] Given the growing recognition of the beneficial potential of JNK inhibitors in human health, there is an increasing demand for comprehensive pharmacokinetic studies of these compounds.

A review of the literature revealed that while several articles discuss some PK parameters of IQ-1 and IQ-18, comprehensive data on their biodisposition in rats have not yet been reported. Pharmacokinetic results for IQ-1, including findings from our team, have been described in mice, rats, and rabbits.[15-18] Our previous study in rats revealed low systemic plasma concentrations of IQ-1 following a single oral administration at a dose of 50 mg/kg in a 1% starch solution.[16] This is likely due to the inherently low aqueous solubility of the compound, which restricts its dissolution in intestinal fluid and consequently limits absorption. Furthermore, the pharmacokinetic parameters of IQ-1 in rats demonstrated dose proportionality within the 50–100 mg/kg dose range, whereas its pharmacokinetics was not dose proportional over the range of 25–50 mg/kg.[18]

It is known that investigation of metabolite pharmacokinetics is a critical component of preclinical and clinical research, particularly when the therapeutic efficacy of the parent compound is mediated by its metabolites. A comprehensive assessment of key metabolite pharmacokinetic parameters – such as exposure in plasma and tissues – is therefore essential to establish a clear exposure-response relationship. Consequently, monitoring metabolite kinetics provides crucial insight into the mechanism of action of the drug and enables an indirect assessment of its efficacy.[19,20]

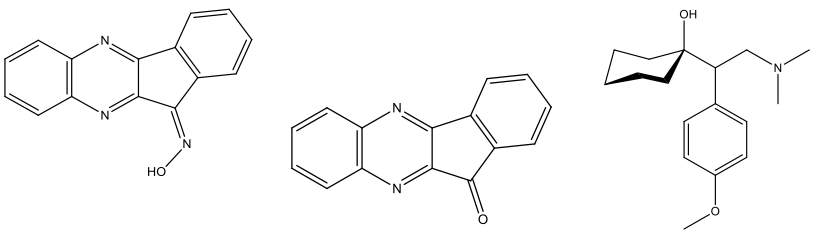
Although the JNK-inhibiting activity of the metabolite IQ-18 has not been demonstrated in previous studies,[8,11,15] its pharmacological profile requires further investigation. Among known compounds, tryptanthrin-6-oxime (TRYP-Ox) and its metabolite tryptanthrine (TRYP) are the closest structural analogs of IQ-1 and its metabolite IQ-18, respectively. Previous in vitro studies have demonstrated that both TRYP-Ox and TRYP are equally potent in suppressing the clinical signs and tissue injury associated with rheumatoid arthritis.[21] We hypothesize that, similar to TRYP, IQ-18 may also exhibit some valuable therapeutic effects. Preliminary data from a rat model of middle cerebral artery occlusion indeed suggest that IQ-18 possesses significant pharmacological activity [unpublished data].

Considering the potential pharmacological activity of the metabolite IQ-18, this study comprehensively investigated the plasma pharmacokinetics and tissue distribution of both the parent compound, IQ-1, and its major metabolite IQ-18 in rats following a single oral dose of IQ-1 (50 mg/kg). To elucidate the absorption pathways and sites of metabolism, we quantified both analytes in lymph, plasma from the hepatic portal vein (HPV) and inferior vena cava (IVC), as well as in bile and intestinal wall samples.

Methods

Chemicals and reagents

The compounds IQ-1 (11*H*-indeno[1,2-*b*]quinoxalin-11-one oxime) and IQ-18 (11*H*-indeno[1,2-*b*]quinoxalin-11-one) were synthesized at the Kizhner Research Center of Tomsk Polytechnic University (Tomsk, Russia), as described previously.[8] The chemical structures (Figure 1) were confirmed by mass spectrometry and NMR; with a sample purity of 99.9%.[8] Venlafaxine (≥98%, Sigma-Aldrich, USA;



a b c

Figure 1. Chemical structures of 11*H*-indeno[1,2-*b*]quinoxalin-11-one oxime (IQ-1) (a), its metabolite 11*H*-indeno[1,2-*b*]quinoxalin-11-one (IQ-18) (b), and venlafaxine (c).

Figure 1) was used as an internal standard (IS).

Diethyl ether (≥ 99%, Kuzbassorghim, Russia), heparin sodium (5000 IU/mL, Belmedpreparaty, Russia), ethyl acetate (≥ 99.7%, ECOS-1, Russia), dimethyl sulfoxide (DMSO, ≥ 99.5%, Reakhim, Russia), ammonium sulfate (≥ 99%, Khimreaktivsnab, Russia), ammonium formate (≥ 99%, Sigma-Aldrich, USA), acetonitrile (≥ 99.9%, Cryochrom, Russia), formic acid (98%, Fluka Analytical, Germany), and 0.9% saline (Gematech, Russia) were used in the study. Ultrapure water was prepared using a Milli-Q Direct-Q 5 UV system (Millipore, USA).

Equipment and instrumentation

The quantification of analytes in biological samples was performed using a LC-20 Prominence analytical system (Shimadzu Corp, Japan) and a mass spectrometer 3200 QTRAP (AB Sciex, USA) equipped with an electrospray ionization source. The liquid chromatography unit comprised a controller module, a DGU-20A3 degasser, an LC-20AD binary pump, a CTO-20A column oven, and a SIL-20A autosampler.

A handheld homogenizer MT-30K (Handzhou Miu Instruments Co., China), a multi-speed vortex MSV-3500 (Biosan, Latvia), and a multifunctional centrifuge SL 16R with cooling (Thermo Scientific, USA) were used for sample preparation.

Standard solutions

Stock solutions of IQ-1 and IQ-18 (1 or 2 mg/mL) were prepared in ACN: DMSO (8:2, v/v) under heating (36 ± 1°C). Working solutions (1, 20, 50, 200, 1000 and 2000 µg/mL) were obtained by diluting the stock solution mixture with 70% ACN. All stock and working solutions were stored at −32°C in amber glass flasks.

Standard calibration solutions (6–8 concentration levels per matrix) in the range of 0.02–800 µg/mL were prepared by diluting working solutions with 70% ACN. Quality control (QC) solutions in four levels (LLOQ, LQC, MQC and HQC) per each matrix were also prepared in 70% ACN (concentration levels are listed in Tables S1 and S2). The internal standard (IS) solution (5000 ng/mL venlafaxine in 70% ACN) was used. Calibration and QC solutions were stored at 4°C in transparent polypropylene microtubes. For QC preparation, separate stock and working solutions of IQ-1 and IQ-18 were used.

Animals and ethics

All animal experiments were conducted in accordance with Directive 2010/63/EU.[22] The protocol was approved by the Institutional Animal Care and Use Committee (IACUC) of the Goldberg Research Institute of Pharmacology and Regenerative Medicine (protocol No. 200A052022). All procedures involving animals were performed under diethyl ether anesthesia. CO_2 was used for euthanasia.

Experimental design

Male Wistar rats (230-260 g) were randomly assigned to groups, as detailed below. All rats were orally administered IQ-1 at a single dose of 50 mg/kg. The animals were housed in plastic cages (57 × 36 × 20 cm) with sawdust bedding under standard conditions (ambient temperature 22 ± 2°C, 40-60% relative humidity, and a 12-h light/12-h dark cycle). Standard rodent chow and water were provided *ad libitum*.

In Stage 1, the plasma pharmacokinetics and tissue distribution of IQ-1 and its metabolite IQ-18 were investigated following a single oral administration of IQ-1 to rats. Blood (from the carotid artery) and tissue samples were collected at 0.5, 1, 2, 4, 6, 8, 15, 24, 30, and 48 h post-dose (n = 50; 5 animals per time point). Both analytes were quantified in biological samples using LC-MS/MS, and pharmacokinetic parameters were subsequently calculated.

In Stage 2, a separate cohort of rats (n = 25; 5 animals per time point) was used to determine the concentrations of IQ-1 and IQ-18 in lymph and plasma (from the HPV and IVC) at 1, 2, 4, 6, and 8 h following a single oral dose of IQ-1. To assess the involvement of both the portal and lymphatic systems in the absorption of IQ-1, its concentrations in the HPV and lymph were compared. Additionally, both analytes were quantified in the IVC and the HPV to estimate concentration changes following hepatic passage.

In Stage 3, we aimed to estimate whether biliary excretion is the primary source of the intestinal IQ-18. For this purpose, a separate group of rats (n = 5) received an oral dose of IQ-1 (50 mg/kg) and underwent bile duct catheterization with exteriorization to divert bile from the intestine. IQ-1 and IQ-18 were quantified in the bile and the intestinal wall at 1 h post-dose.

Preparation of the drug formulation and dosing

The oral formulation of IQ-1 was prepared fresh for each experimental group. A precisely weighed quantity of IQ-1 was triturated with 0.9 mL of Tween-80 using a pestle and mortar until a homogeneous, creamy suspension was obtained. This mixture was then gradually diluted with 5 mL of a 1% starch solution. Rats received a single 50 mg/kg oral dose via intragastric gavage.

Sample collection and preparation

In Stage 1, blood samples were collected from the right carotid artery at predetermined time points (0.5, 1, 2, 4, 6, 8, 15, 24, 30, and 48 h post-dose), placed into heparinized plastic tubes (15 IU heparin/mL) and centrifuged at 1700 g for 10 min at 4°C to separate the plasma. Immediately after blood collection, the liver was perfused with ice-cold normal saline via the HPV, with drainage through the IVC. Subsequently, the animals were sacrificed, and tissues (liver, kidneys, heart, brain, lungs, spleen, skeletal muscles, adipose tissue, and duodenum) were immediately excised. All tissues were gently rinsed with ice-cold normal saline and blotted dry with filter paper on an ice-cold surface. The heart was perfused via the aorta with 10 mL of ice-cold normal saline to eliminate residual blood. The time between the collection of biological samples and storage at −80°C was maintained within 10 min to avoid stability-related issues.

In Stage 2, lymph samples (100 µL) were collected from

the mesenteric lymph duct at 1, 2, 4, 6, and 8 h post-dose without cannulation. To facilitate visualization of the lymphatic duct, rats received 2 mL of 5% milk orally 10 min prior to anesthesia. The duct was punctured using a syringe needle, and passively flowing lymph was collected over 10 min into a heparinized tube. Collection was performed using a heparin-rinsed glass capillary (ID = 1.0 mm) connected to a vacuum pump (5 cmHg) via silicone tubing. Immediately following lymph collection, blood samples were obtained through direct puncture of the HPV and IVC using heparinized 3 mL syringes with 21 G needles. Plasma was separated by centrifugation.

In Stage 3, after a single oral dose of IQ-1 followed by bile diversion from the intestine, bile samples (100 µL) were collected at 1 h post-dose via bile duct catheterization from restrained rats under diethyl ether anesthesia. Following bile collection, 10-cm duodenal segments were immediately excised and extensively rinsed with normal saline (three washes) to ensure complete removal of residual luminal content.

All plasma, tissue, lymph, and bile samples were stored at −80°C until analysis. Prior to extraction, frozen samples were thawed to room temperature. Tissue samples (285 mg) were homogenized in 3 M ammonium sulfate solution (by two 30-sec homogenization cycles, with the addition of 0.25 mL per cycle) using a hand-held homogenizer. A liquid-liquid extraction method using ethyl acetate with ammonium sulfate as a desalting agent was applied to sample preparation.

For plasma samples, a working solution of the IS (30 µL), 3 M ammonium sulfate (300 µL), and ethyl acetate (780 µL) were sequentially added to 2.0 mL polypropylene centrifuge tubes containing 300 µL of spiked rat plasma. For bile and lymph samples (100 µL), the volume of the added IS was adjusted to 10 µL. The samples were vortex mixed for 2 min at 2100 rpm and then separated by centrifugation at 12,000 g for 8 min at 4°C. The organic supernatant (740 µL) was transferred into new 1.5-mL polypropylene centrifuge tubes and evaporated to dryness under a nitrogen stream at room temperature. Finally, the residue was reconstituted in acetonitrile (300 µL), vortexed for 5 min at 1200 rpm, and transferred into vials for analysis.

To extract analytes from tissues, the working solution of the IS (30 µL) was added to 2.0 mL polypropylene centrifuge tubes containing the tissue homogenate (300 mg in 0.5 mL of 3 M ammonium sulfate). The samples were vortex mixed at 1000 rpm for 7 min. Subsequently, ethyl acetate (1.2 mL) was added to the mixture, and samples were vigorously vortexed at 2100 rpm for 10 min. After centrifugation at 12,000 g for 8 min at 4°C, the organic layer was either analyzed directly without drying (for adipose tissue) or transferred into a 1.5-mL polypropylene tube and evaporated to dryness under a nitrogen stream at room temperature (for all other tissue samples). The residue was then reconstituted in acetonitrile (300 µL), vortexed for 5 min at 1200 rpm, and transferred into vials for analysis.

Validation of the method and determination of IQ-1 and IQ-18 in rat biosamples

The determination of IQ-1 and IQ-18 in rat biosamples was performed using a previously described LC-MS/MS method with venlafaxine as the IS.[16] The analytical method has previously been validated in rat plasma according to the European Medicines Agency (EMA) guidelines in terms of selectivity, sensitivity, linearity, accuracy, precision, carry-over, recovery, matrix effect, stability, and dilution integrity.[23] This method has been shown to be suitable for the simultaneous quantitative analysis of IQ-1 and metabolite IQ-18 in rat plasma.[16] In the present work the validation procedures were carried out in rat tissues, bile, and lymph.

Selectivity and linearity were assessed in plasma, tissues (liver, kidney, heart, brain, lung, spleen, muscle, fat, and duodenum), lymph, and bile. The selectivity of the method was investigated by analyzing six individual blank samples. To evaluate linearity, calibration curves were constructed by plotting the peak area ratio (y) of the analyte to the IS against the corresponding concentration (x) of the analyte using a $1/x^2$ weighted least-squares linear regression model.

Calibration samples were prepared using biosamples from intact rats. For constructing calibration curves, different ranges of standard solutions were used for each type of biological sample. The final concentration ranges for each matrix are listed in the Table 1. For the plasma analysis, calibration samples were prepared by freshly spiking the calibration solutions (15 µL) with the IS (30 µL) and blank plasma (285 µL). For the analysis of lymph and bile, the calibration solutions (5 µL) were spiked with the IS (10 µL) and blank lymph/bile (95 µL). For analysis of tissue samples, calibration standards (15 µL) were spiked with the IS (30 µL) along with tissue homogenate (0.285 g

Table 1. Linear ranges, equations, and correlation coefficients (R) for IQ-1 and IQ-18 in different matrices.

Sample	Analyte	Linear ranges	Equations	R
Brain	IQ-1	1.5-2250 ng/g	y=7.59e-4x+0.0017	0.9932
	IQ-18	1.5-6000 ng/g	y=2.075e-4x+0.00034	0.9960
Heart	IQ-1	1.5-2250 ng/g	y=11.4e-4x+0.0373	0.9921
	IQ-18	1.5-2250 ng/g	y=3.06e-4x+0.0021	0.9955
Liver	IQ-1	1.5-9000 ng/g	y=8.44e-4x+0.0374	0.9955
	IQ-18	1.5-9000 ng/g	y=10.00e-4x+0.0017	0.9942
Kidney	IQ-1	1.5-3000 ng/g	y=47.60e-4x+0.0187	0.9985
	IQ-18	1.5-3000 ng/g	y=15.50e-4x-0.0056	0.9943
Lung	IQ-1	1.5-3000 ng/g	y=5.91e-4x+0.0093	0.9984
	IQ-18	1.5-3000 ng/g	y=1.66e-4x+0.0004	0.9950
Spleen	IQ-1	1.5-1500 ng/g	y=12.90e-4x+0.0156	0.9968
	IQ-18	1.5-1500 ng/g	y=3.54e-4x-0.0009	0.9912
Muscle	IQ-1	1.5-3000 ng/g	y=19.10e-4x+0.0153	0.9975
	IQ-18	1.5-2250 ng/g	y=3.725e-4x+0.00165	0.9977
Fat	IQ-1	1.5-1500 ng/g	y=8.66e-4x+0.0017	0.9936
	IQ-18	1.5-3000 ng/g	y=1.94e-4x+0.0003	0.9955
Duodenum	IQ-1	1.5-6000 ng/g	y=10.00e-4x+0.0211	0.9924
	IQ-18	1.5-6000 ng/g	y=2.00e-4x+0.0017	0.9970
Plasma	IQ-1	1-4000 ng/mL	y=13.00e-4x+0.0180	0.9943
	IQ-18	1-4000 ng/mL	y=9.28e-4x+0.0002	0.9952
Lymph	IQ-1	1-4000 ng/mL	y=9.68e-4x+0.0071	0.9930
	IQ-18	1-4000 ng/mL	y=1.57e-4x-0.0001	0.9963
Bile	IQ-1	1-4000 ng/mL	y=1.12e-4x-0.0007	0.9976
	IQ-18	1-20000 ng/mL	y=1.89e-4x+0.0004	0.9980

tissue in 0.5 mL of 3 M ammonium sulfate). Blank and zero samples were prepared using 70% ACN (15 µL) instead of the calibration solutions or QCs.

Analytes in unknown samples were quantified using calibration curves generated within the same analytical run. The calibration curves were constructed by plotting the peak area ratio of each analyte (IQ-1 or IQ-18) to the IS against the nominal concentration of spiked calibration standards (expressed as ng/mL or ng/g).

LC System

Chromatographic separation was performed using an EC Nucleodur C8 ec LC column (150 × 4.6 mm, 5 µm) (Macherey-Nagel, Germany) coupled with a precolumn cartridge at 40°C.

Mobile phase A (5 mM ammonium formate and 0.1% formic acid (v/v) in water, pH = 2.9) and mobile phase B (acetonitrile) were delivered at a flow rate of 0.6 mL/min under gradient conditions, as previously described.[9] The total run time was 10.0 min. The autosampler was maintained at 15°C. The injection volume was 2 µL.

The mass spectrometer operated in positive ion mode with unit mass resolution. MS/MS detection was performed using multiple reaction monitoring mode with transitions at m/z 248.3 → 131.0 for IQ-1, 233.2 → 103.1 for IQ-18 and 278.0 → 58.0 for the IS. The parameters for the electrospray ionization source were as follows: ion source temperature of 550°C, curtain gas (nitrogen) at 15 psi, nebulizer gas (air) at 60 psi, heater gas (air) at 25 psi, ion spray voltage of 3500 V, and interface heater at 100°C.

Pharmacokinetic data analysis

Data acquisition and analysis were carried out using Analyst 1.6 software (AB Sciex, USA) and MultiQuant 2.1 (AB Sciex, USA), respectively. Noncompartmental analysis of pharmacokinetic parameters was performed using WinNonlin software (version 5.2, Pharsight Corporation, USA).[24]

The maximal concentration (C_{max}) and the time to maximal concentration (T_{max}) were determined directly from the plasma concentration–time profiles. The elimination rate constant (K_{el}) was calculated by regression analysis of the logarithmically transformed terminal linear portion of the concentration–time curve, using 3–4 data points from this segment; the correlation coefficient (R) exceeded 0.99. The elimination half–life ($T_{1/2}$) was derived from the formula of $0.693/K_{el}$. The area under the concentration–time curve from time zero to the last measurable concentration (AUC_{0-t}) was calculated using the linear/log trapezoidal method, from time 0 to T_{last}. The area under the curve extrapolated to infinity ($AUC_{0-\infty}$) was calculated by the linear/log trapezoidal method from time 0 to $T_{last,}$ with extrapolation from T_{last} to infinity based on the observed concentration at the last time point divided by the terminal elimination rate constant (K_{el}).

Total clearance (Cl/F) was calculated as: administrated Dose/$AUC_{0-\infty}$. Mean residence time (MRT_{0-t}) was calculated as $AUMC_{0-t}/AUC_{0-t}$, where $AUMC$ represents the area under the first moment curve formed by product of concentration and time. The volume of distribution (V_d/F) was calculated as $(Cl/F)/K_{el}$. The extrapolated area under the concentration-time curve (AUC_{extrap}) was estimated as a percentage of $AUC_{0-\infty}$ due to extrapolation from time of last measurable positive concentration: $(AUC_{0-\infty} - AUC_{0-t})/AUC_{0-\infty} \times 100$. Finally, the tissue-to-plasma partition coefficient (K_p), was calculated as the ratio: tissue AUC_{0-t}/plasma AUC_{0-t}.

Statistical analysis

Parameters were analyzed by descriptive statistics using the Statistica software package (version 12, USA) and presented as the mean ± standard deviation (SD). The comparison of PK parameters was performed by the nonparametric Mann–Whitney U test. A difference between the compared values was considered significant at $P < 0.05$.

Results

Validation

The results of selectivity assessment indicate that any endogenous matrix did not interfere with the detection of IQ-1, IQ-18 and IS. As a result of sensitivity tests, the LLOQ was determined to be 1 ng/mL (lymph, bile) or 1.5 ng/g (other matrices) with the signal-to-noise ratio more than 10. Validation results indicate that the LC–MS/MS method can be applied for the determination of IQ-1 and metabolite IQ-18 at a low concentration level in rat biosamples.

The calibration curves demonstrated good linearity over the tested concentration ranges. Linear ranges, regression equations, and the correlation coefficients are listed in Table 1.

All results of within-run and between-run accuracy for IQ-1 and metabolite IQ-18 were within the acceptable limits (in the range of 88-110%; Table S1 and S2, Supplementary material). These results confirm that the method enables accurate and precise quantitation of IQ-1 and metabolite IQ-18 in the studied concentration ranges. Carry-over was not observed.

The extraction recovery and matrix effects for both analytes were within acceptable criteria for all biological samples (the mean extraction recoveries ranged from 88% to 94%; Table S3, S4).

The IS-normalized matrix factors for IQ-1 and IQ-18 were in the range of 0.81–1.23 indicating that endogenous substances did not cause interference at the retention time of analytes.

Previously, IQ-1 was determined to be unstable in plasma samples under both short-term and long-term storage at −32°C, whereas IQ-18 remained stable under the same conditions[16]. Consequently, the present study modified storage conditions to −80°C. Data on the stability of analytes in rat biosamples are presented in Table S3 and S4 (Supplementary material).

Plasma pharmacokinetics

Following a single oral 50 mg/kg dose, IQ-1 and metabolite IQ-18 were detected in plasma up to 24 h and 48 h post-

dose, respectively. The plasma concentration-time curves are presented in Figure 2 (a, b). Noncompartmental PK parameters are summarized in Table 2.

Following oral administration, IQ-1 exhibited rapid absorption with a T_{max} of 1 h, relatively low C_{max} (59.69 ± 13.97 ng/mL), and an elimination half-life ($T_{1/2}$) of 5.58 h. IQ-1 is metabolized into IQ-18. Concentrations of IQ-18 remained below 50 ng/mL within 2 h after dosing. The metabolite demonstrated prolonged attainment of maximal concentrations, with the C_{max} values reached at 8 h post-dose (Table 2). The rise in IQ-18 levels by 4 h post-dose indicates an active biotransformation process for IQ-1, a conclusion further supported by its high clearance rate (Table 2). The V_d/F for IQ-1 greatly exceeded the total body water volume in rats (~668.0 mL/kg), which is characteristic for extensive tissue distribution. IQ-18 exhibited a significantly longer $T_{1/2}$ and $MRT_{0\text{-}t}$ than IQ-1 ($P < 0.05$). The plasma $AUC_{0\text{-}t}$ for IQ-18 was 96-fold higher than that for IQ-1.

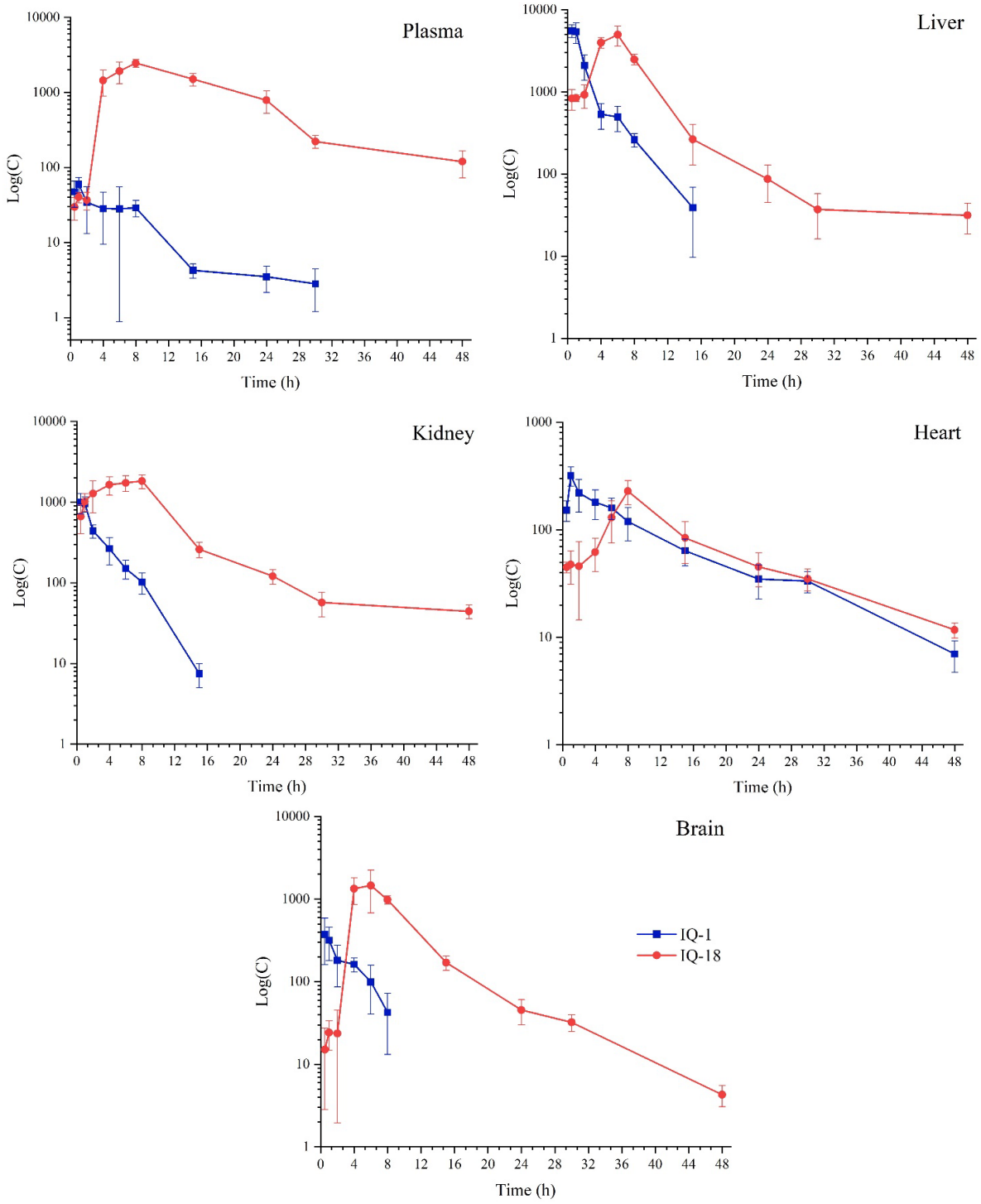


Figure 2. Concentration-time profiles of IQ-1 and IQ-18 in rat plasma and tissues (liver, kidney, heart, and brain) following a single oral dose of IQ-1 (50 mg/kg). Values are expressed as mean concentration (ng/mL in plasma, ng/g in tissues) ± standard deviation, n = 5 per each time point.

Table 2. Noncompartmental pharmacokinetic parameters of IQ-1 and IQ-18 following a single oral administration of IQ-1 at a dose of 50 mg/kg.

Matrix	Analyte	PK parameters										
		T_{max}, h	C_{max}, ng/g	AUC_{0-t}, ng·h/g	$AUC_{0-\infty}$, ng·h/g	AUC_{extrap}	$T_{1/2}$, h	K_{el}, 1/h	MRT_{0-t}, h	Cl/F, L/(h·kg)	V_d/F L/kg	K_p
Liver	IQ-1	0.50	5540.15	13337.33	13474.80	1.02	2.44	0.28	2.50	-	-	32.29
	IQ-18	6.00	4960.81	35004.60	35519.91	1.45	11.36	0.06	7.40	-	-	0.88
Kidney	IQ-1	0.50	995.04	3196.42	3220.15	0.74	2.20	0.31	3.22	-	-	7.74
	IQ-18	8.00	1829.71	22088.87	22942.09	3.72	13.33	0.05	8.93	-	-	0.56
Brain	IQ-1	0.50	374.80	1265.66	1428.17	11.38	2.64	0.26	2.93	-	-	3.06
	IQ-18	6.00	1460.27	12202.86	12236.30	0.27	5.39	0.13	8.67	-	-	0.31
Heart	IQ-1	1.00	317.96	3099.42	3205.02	3.29	10.43	0.07	12.13	-	-	7.50
	IQ-18	8.00	228.50	3077.75	3276.87	6.08	11.77	0.06	15.07	-	-	0.08
Lung	IQ-1	1.00	1249.41	3401.72	3518.89	3.33	3.41	0.2	3.42	-	-	8.24
	IQ-18	6.00	840.96	11790.34	14277.70	17.42	21.70	0.03	14.09	-	-	0.30
Spleen	IQ-1	0.50	424.99	1935.50	1945.44	0.51	1.81	0.38	3.30	-	-	4.69
	IQ-18	4.00	356.66	3507.29	3992.47	12.15	20.08	0.03	11.48	-	-	0.09
Muscles	IQ-1	0.50	531.37	724.39	835.05	13.25	5.83	0.12	3.09	-	-	1.75
	IQ-18	6.00	408.72	3506.77	3657.92	4.13	14.08	0.05	9.19	-	-	0.09
Fat	IQ-1	0.50	719.40	3197.88	3218.05	0.63	6.69	0.1	6.58	-	-	7.74
	IQ-18	8.00	1395.58	17508.98	18940.49	7.56	13.85	0.05	12.43	-	-	0.44
Plasma*	IQ-1	1.00	59.69	413.07	441.25	6.39	5.58	0.12	6.43	113.32	912.15	-
	IQ-18	8.00	2464.06	39592.87	41126.60	3.73	8.88	0.08	14.58	-	-	-

Parameters were estimated using WinNonlin software (version 5.2). Data are presented as mean values (n = 5 per each time-point). For the marked matrices (*) C_{max} values are expressed in ng/mL, AUC_{0-t} and $AUC_{0-\infty}$ values - in ng·h/mL. K_p values are calculated by the formula: AUC_{0-t} (tissue)/AUC_{0-t} (plasma).

Tissue distribution

The concentration-time curves of IQ-1 and its metabolite IQ-18 in various tissues following a single oral dose of IQ-1 are presented in Figures 2 and 3. IQ-1 was detectable in the brain and spleen for up to 8 h, while it was found in most other tissues for up to 15 h post-dose. In the liver and heart, IQ-1 was measurable for up to 30 h and 48 h, respectively. IQ-18 was detected in most tissues for up to 48 h post-dose, except for the muscles and brain where it was measurable for up to 30 h post-dose.

Pharmacokinetic parameters for IQ-1 and IQ-18 in tissues, calculated using the non-compartmental method, are summarized in Table 2. The maximal concentrations of IQ-1 in all tissues were reached at 0.5 or 1 h (T_{max}) and significantly exceeded the corresponding plasma C_{max}. IQ-1 was quickly transferred from the serum to the investigated tissues and demonstrated high tissue affinity. The metabolite IQ-18 also showed wide tissue distribution, with longer T_{max} values of 4 h (spleen), 6 h (liver, brain, lung, and muscles), and 8 h (kidneys, heart, and fat), indicating slower tissue distribution compared to the parent compound (IQ-1).

The highest concentrations of IQ-1 and IQ-18 were detected in the liver, with C_{max} values of 5.54 and 4.96 µg/g, respectively (Table 2). Based on the MRT_{0-t} values, organs can be ranked in descending order as follows: heart > fat > lungs > spleen > kidneys > muscles > brain > liver (IQ-1); heart > lungs > fat > spleen > muscles > kidneys > brain > liver (IQ-18). The elimination half-life ($T_{1/2}$) of IQ-1 varied from 1.81 h (spleen) to 10.43 h (heart), while that of the metabolite IQ-18 ranged from 5.39 h (brain) to 21.70 h (lungs).

For IQ-1, the areas under the pharmacokinetic curve in tissues exceeded those in plasma (the tissue-to-plasma partition coefficient $K_p > 1$), indicating extensive tissue distribution. Based on the K_p values, the tissue tropism of IQ-1 and IQ-18 can be presented in descending order as follows liver > lung > kidney, fat > heart > spleen > brain > muscles (IQ-1); liver > kidneys > fat > brain, lung > spleen, muscles, and heart (IQ-18). Our results indicate that the primary target for both IQ-1 and its metabolite IQ-18 is the liver, a well-perfused organ with the greatest filtering capacity.

Levels of IQ-1 and IQ-18 in lymph, HPV, and IVC

The concentrations of both analytes and *AUC* values in lymph and plasma (obtained from both the HPV and IVC) were compared (Table 3, 4). The reduction of both analytes during hepatic passage was evaluated using their HPV/IVC concentration ratios.

IQ-1 concentrations in lymph remained stable at relatively low levels during the first 2 h post-dose compared to the corresponding HPV levels. The mean concentrations of IQ-1 in the HPV were 3.5-, 4.2-, and 6.7-fold higher than in the lymph at 1, 2, and 4 h, respectively. For IQ-1 and IQ-18, the *AUCs* in the HPV were 4-fold and 6.9-fold higher, respectively, than those in lymph. These findings may indicate that both intestinal lymphatic and portal systems contribute to the absorption of IQ-1. We propose that the portal route (HPV) is the predominant pathway for drug transport.

Furthermore, concentrations of IQ-1 in the HPV from 1 h to 8 h post-dose were significantly higher than the

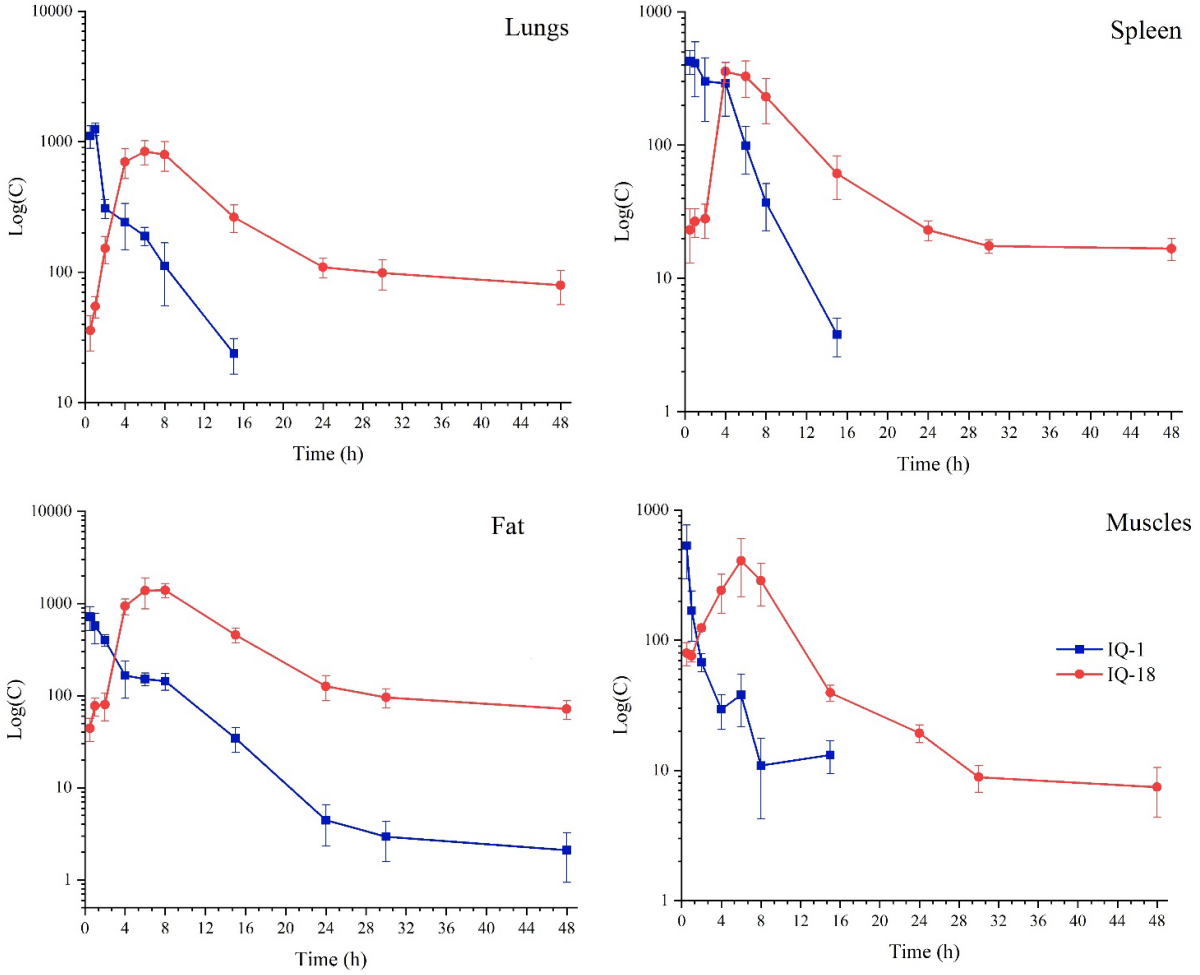


Figure 3. Concentration-time profiles of the parent compound (IQ-1) and its metabolite (IQ-18) in rat tissues (lungs, spleen, fat, muscles) following a single oral administration of IQ-1 at a dose of 50 mg/kg. Values are expressed as mean concentration (ng/g) ± standard deviation, n = 5 per each time point.

Table 3. Concentrations and $AUC_{0\text{-}t}$ of IQ-1 in the HPV, IVC, and lymph following a single oral administration of IQ-1 to rats at a dose of 50 mg/kg.

Time post-dose, h	HPV	IVC	Lymph
1	813.12 ± 170.15	37.96 ± 4.23	235.2 ± 51.4
2	839.56 ± 86.08	36.86 ± 6.28	201.7 ± 32.6
4	936.64 ± 256.47	13.68 ± 3.60	140.0 ± 25.0
6	193.34 ± 65.76	8.63 ± 1.29	111.3 ± 12.2
8	80.63 ± 19.94	7.52 ± 1.47	59.5 ± 17.3
$AUC_{0\text{-}t}$ (ng·h/mL)	4413.05	145.39	1099.85

Values are expressed as mean ± standard deviation (n = 5 per each time point).

Table 4. Concentrations and $AUC_{0\text{-}t}$ of IQ-18 in the HPV, IVC, and lymph following a single oral administration of IQ-1 to rats at a dose of 50 mg/kg.

Time post-dose, h	HPV	IVC	Lymph
1	16.85 ± 1.50	10.91 ± 0.94	19.4 ± 4.6
2	60.07 ± 4.68	11.31 ± 1.09	16.6 ± 3.8
4	747.30 ± 135.88	188.41 ± 33.35	47.4 ± 17.2
6	1629.07 ± 232.89	809.67 ± 100.46	120.2 ± 33.7
8	2285.41 ± 82.88	1461.28 ± 217.96	655.6 ± 149.6
$AUC_{0\text{-}t}$ (ng·h/mL)	7145.10	3485.31	1035.10

Values are expressed as mean ± standard deviation (n = 5 per each time point).

corresponding levels in the IVC ($P < 0.05$). Similarly, IQ-18 levels in the HPV at 4, 6, and 8 h post-dose exceeded those in the IVC by factors of 4, 2, and 1.6, respectively ($P < 0.05$; Table 4). For IQ-1 and IQ-18, the *AUCs* in the HPV were > 30-fold and 2-fold higher, respectively, than those in the IVC. These results may indicate that the levels of both compounds in venous blood were substantially reduced following hepatic passage.

Levels of IQ-1 and IQ-18 in the bile and intestinal wall

Concentration of IQ-1 in the bile was 336.92 ± 93.45 ng/mL. Levels of the metabolite IQ-18 in the bile were quite high (927.62 ± 158.75 ng/mL), significantly exceeding its corresponding plasma levels.

Concentrations of both IQ-1 and IQ-18 in the intestinal wall (duodenum) at 1 h post-dose are presented in Table 5. Analysis of the intestinal wall (duodenum) following a single oral dose of IQ-1 (without bile diversion) revealed substantial concentrations of both IQ-1 and IQ-18 at 1 h post-dose (Table 5). When biliary diversion was implemented, the concentration of IQ-18 in intestinal wall decreased significantly ($P < 0.05$) compared to the group without bile diversion (Table 5). In contrast, the concentration of IQ-1 was not significantly

Table 5. Concentrations of IQ-1 and IQ-18 in rat intestinal wall (duodenum) at 1 h after a single oral administration of IQ-1 at a dose of 50 mg/kg.

Analyte	Without bile diversion, ng/g	With bile diversion, ng/g
IQ-1	3159.96 ± 999.08	2658.22 ± 472.99
IQ-18	2198.99 ± 1018.12	89.99 ± 2.35*

Values are expressed as mean ± standard deviation (n = 5 per group). * - statistically significant changes compared to the group without bile diversion

affected (Table 5). These data demonstrate that the high concentration of the metabolite IQ-18 in the duodenum originates from the bile. These findings indicate that the intestinal wall participates in the biotransformation of IQ-1, but it is not the primary site of metabolism. Presumably, the compound is predominantly metabolized in the liver with subsequent biliary excretion into the gastrointestinal tract.

Discussion

In the present study, we aimed to investigate the pharmacokinetic characteristics of 11*H*-indeno[1,2-*b*] quinoxalin-11-one oxime (IQ-1) and its metabolite 11*H*-indeno[1,2-*b*]quinoxalin-11-one (IQ-18) in rats following a single oral dose of IQ-1 (50 mg/kg).

It is widely accepted that the chemical nature and physicochemical properties of a substance play a crucial role in its oral bioavailability.[25,26] Based on its physicochemical characteristics (lipophilicity coefficient logP = 3.29, ionization constant pKa = 8.90, molecular weight 247.07 g/mol, polar surface area tPSA = 57.31), IQ-1 is expected to be well absorbed. However, strong intermolecular interactions within the crystal lattice, combined with its rigid structure, hinder the dissolution of the compound in aqueous environments, thereby reducing its absorption through the gastrointestinal tract.[27] The low systemic exposure is consistent with the previously reported bioavailability of IQ-1 in rats, which was less than 1.5% across a dose range of 25 to 100 mg/kg administered orally in a starch mucus formulation.[18] In the present work, we assessed the previously unstudied biodisposition of IQ-1 and IQ-18 in rats, elucidated the absorption pathways of IQ-1 and its possible sites of metabolism.

Analysis of plasma pharmacokinetics in the present work revealed that IQ-1 is quickly absorbed (T_{max} = 1 h), with maximal concentrations remaining below 60 ng/mL. These low plasma levels are likely due to metabolism and extensive plasma protein binding (approximately 55%; our unpublished data). The rise in mean plasma IQ-18 concentration from 2 h to a peak at 8 h post-dose demonstrates the gradual metabolism of IQ-1. We have found large differences in concentrations between the parent compound, IQ-1, and the metabolite, IQ-18, in plasma and tissues. The C_{max} of metabolite IQ-18 in systemic circulation (carotid artery plasma) was 41-fold higher than that of the parent compound. Notably, IQ-18 exhibited significantly different absorption and elimination rates compared to IQ-1. Namely, the calculated plasma T_{max} for IQ-1 and IQ-18 were 1 h and 8 h, respectively. Presumably, this 7-h delay for IQ-18 compared to IQ-1 is attributed to the absorption of the metabolite from the intestine following its biliary excretion. Furthermore, the possible extrahepatic metabolism of IQ-1 (in organs) may represent an additional source of systemic IQ-18. The elimination rate constant (K_{el}) of metabolite IQ-18 was 1.6-fold higher than that of IQ-1. High total clearance *Cl/F* and apparent volume of distribution (V_d/F) observed for IQ-1 in plasma are consistent with its extensive tissue distribution. In plasma and most tissues, IQ-18 demonstrated a longer elimination half-life ($T_{1/2}$) and a larger area under the curve (AUC_{0-t}) than IQ-1, although these parameters for both compounds were similar in heart tissue. These findings indicate that the elimination of IQ-18 is a slower process, leading to its longer retention in the organism compared to the parent compound. Consequently, the plasma concentration of IQ-18 does not decline but increases over the first 8 h post-dose, with most of the administered IQ-1 being eliminated by the time the metabolite reaches its peak concentration.

Our experiments have demonstrated, that IQ-1 and IQ-18 are distributed to all investigated tissues. The C_{max} of IQ-1 in tissues substantially exceeded its plasma levels. For IQ-18, the C_{max} in the liver was higher than its plasma C_{max}, and the AUC_{0-t} values in the liver and plasma were similar. Moreover, we observed similar C_{max} of both analytes in the liver, while in many organs (the heart, lungs, spleen, and muscles) the C_{max} values of the parent compound, IQ-1, even exceeded those of its metabolite, IQ-18. According to the C_{max} and K_p, both the parent compound and its metabolite IQ-18 exhibit the highest affinity for the liver.

A comparative analysis showed that the tryptanthrin-6-oxime (TRYP-Ox) and tryptanthrin (TRYP) are structurally the most similar to IQ-1 and IQ-18, respectively. According to the literature, pharmacokinetic studies of TRYP-Ox following oral administration have been conducted in Sprague-Dawley rats[28,29] and Kunming mice.[30] Similar to our results, following an 80 mg/kg oral dosing to mice, the authors have also demonstrated quick absorption of the substance with a similar plasma T_{max} (1.5 h), a long terminal phase, fast and vast tissue distribution with the highest values found in the liver.[30] However, the T_{max} values in murine tissues were much higher (2.5 h)[30] compared to the corresponding values in rats obtained in our study (0.5 h to 1 h post-dose). Compared to the 50 mg/kg dose used in the present study, the higher dose in the previous work[31] could have prolonged the absorption phase.

The pharmacokinetic parameters of the metabolite IQ-18 in rats after an oral dose of IQ-1 were consistent with those reported by other authors for TRYP. Specifically, we observed similar T_{max} (4–8 h for IQ-18 versus 4.6 h to 12 h for TRYP)[28,29] and a comparable *MRT* values across tissues. For example, the *MRT* values for IQ-18 in the liver and spleen were 7.4 h and 11.48 h, respectively; the corresponding values for TRYP were 7.81 h and 11.65 h.[28]

It was previously demonstrated that following oral dosing to rats, TRYP is primarily distributed to tissues with the most abundant blood supply (liver, kidneys, and

lungs)[28] and low concentrations have been detected in the heart that could be associated with its tight binding with some proteins there.[29] The authors assumed that TRYP is metabolized in the small intestine, while the liver might be the main metabolizing organ.[29] This is consistent with our preliminary conclusions on the metabolism of IQ-1.

While the ability of TRYP-Ox to cross the blood-brain barrier (BBB) and exert neuroprotective effects was demonstrated in a rat model of cerebral ischemia-reperfusion,[31] the evidence for TRYP itself is conflicting. In vitro studies confirm that TRYP can cross the BBB.[32] However, in vivo studies following oral administration to rats failed to detect TRYP in the brain, adipose tissue, or muscles, suggesting it has difficulty traversing the BBB in vivo and exhibits poor solubility in fat solvents.[28,29]

In contrast to TRYP, this work demonstrates that both IQ-1 and its metabolite IQ-18 can cross the BBB and penetrate into the brain, which is consistent with the significant neuroprotective effects of IQ-1 observed in murine and rat models of ischemia-reperfusion injury.[9,14] The maximum concentration of IQ-18 in the brain exceeded that of IQ-1 by a factor of 3.9. Furthermore, our study successfully quantified both compounds in adipose tissue and muscles. The tissue-to-plasma partition coefficient for IQ-1 in adipose tissue was 7.74. These data indicate that IQ-1 has a high affinity for adipose tissue, a property shared by many other compounds with a logP > 2 and either acidic or neutral properties.[25]

Furthermore, this study demonstrated that concentrations of IQ-1 in the HPV significantly exceeded those in lymph at 1-6 h post-dose. The total amount of IQ-1 absorbed from the gastrointestinal tract represents the sum of the fractions transported via the lymphatic system and the HPV.[33] Our comparison of IQ-1 concentrations and *AUCs* in the HPV and lymph suggests that portal venous transport may predominate for IQ-1 absorbed from the gastrointestinal tract. Nevertheless, the primary transport pathway cannot be definitively identified. Differences in portal-vein and mesenteric-lymph flow rates also affect drug absorption and must be considered before drawing firm conclusions.

In our work milk was given shortly before lymph sampling to evoke a strong, transient increase in lymph flow. Without this step, lymph collection is technically much more difficult. Although the fat content of milk can alter pharmacokinetics, the physicochemical behavior of the test compound remains the decisive factor. For lipophilic substances (logP > 5), co-administration of fat markedly accelerates gastrointestinal absorption; therefore, milk should be used cautiously in such cases. The test compound, IQ-1, is not lipophilic (logP ≈ 3.29) and is virtually insoluble in the oil phase; any effect of milk on its kinetics is expected to be minimal. Nonetheless, to ensure that the comparison of portal-vein and lymphatic concentrations reflects genuine absorption pathways rather than milk-induced variability, milk was given at a fixed 10-min interval prior to anesthesia.

We hypothesize that IQ-1 entered via the HPV undergoes extensive hepatic first-pass metabolism. In contrast, IQ-1 transported via the lymphatic system bypasses hepatic first-pass metabolism. The fraction of IQ-1 metabolized in the liver was not quantified in the present study. Based on the results obtained, we cannot draw final conclusions about the magnitude of hepatic first-pass extraction. Such quantitative statements require additional experiments.

The detection of the IQ-18 metabolite in duodenal tissue samples under conditions of bile diversion provides evidence for the role of the intestinal wall in the metabolism of IQ-1. No significant difference was found in the intestinal wall concentrations of IQ-1 between the groups with and without bile diversion ($P = 0.765$; Table 4). In contrast, levels of the metabolite IQ-18 decreased dramatically from 2199 ± 1018 ng/g to 90 ± 2 ng/g ($P < 0.05$; Table 4). This striking difference indicates that the intestine is not a major site of IQ-1 metabolism. Instead, IQ-1 appears to be extensively metabolized in the liver, followed by hepatobiliary excretion of its metabolites into the intestinal lumen. This explains the observed 7-h delay in the T_{max} for IQ-18 (8 h) compared to IQ-1 (1 h). Furthermore, additional peaks in the bile chromatogram indicated the presence of other, unidentified metabolites. No clear evidence of enterohepatic circulation was observed under the conditions of this study.[28]

Conclusion

This work presents the first comprehensive investigation of plasma pharmacokinetics and tissue distribution of both IQ-1 and its major metabolite IQ-18 in rats following a single oral dose of IQ-1. We demonstrated that IQ-1 is rapidly absorbed, reaching a C_{max} of approximately 60 ng/mL at 1 h post-dose, and is metabolized into IQ-18. Compared to IQ-1, the metabolite IQ-18 exhibited a considerably longer plasma T_{max} (8 h vs. 1 h) and significantly higher C_{max} (41-fold). The elimination half-life ($T_{1/2}$) of IQ-18 was 1.6-fold longer than that of IQ-1.

Both compounds were widely distributed to tissues, with the highest concentrations and tissue-to-plasma ratios observed in the liver. IQ-1 was found to cross the BBB and exhibit high affinity for adipose tissue. IQ-1 reaches the systemic circulation via both the portal (HPV) and intestinal lymphatic systems. High HPV/IVC concentration ratios suggest that levels of both analytes in venous blood plasma were substantially reduced following hepatic passage. We found that the intestinal wall contributes to the biotransformation of IQ-1, but it is not the primary site of metabolism. High concentrations of IQ-18 in the bile along with its low levels in the intestinal wall after bile diversion strongly indicate that IQ-1 is primarily metabolized in the liver, followed by biliary excretion of IQ-18 into the gastrointestinal tract. Our findings provide a valuable pharmacokinetic foundation for the further development of IQ-1 as a unique drug candidate.

Authors' Contribution

Conceptualization: Galina A. Frelikh, Elena A. Yanovskaya
Data curation: Elena A. Yanovskaya, Galina A. Chernysheva

Formal analysis: Andrei I. Khlebnikov
Methodology: Galina A. Frelikh, Elena A. Yanovskaya, Alexander P. Lakeev, Galina A. Chernysheva, Vera I. Smolyakova
Resources: Andrei I. Khlebnikov
Supervision: Galina A. Chernysheva
Writing–original draft: Galina A. Frelikh
Writing–review & editing: Elena A. Yanovskaya, Alexander P. Lakeev, Galina A. Chernysheva, Vera I. Smolyakova

Competing interests
The authors declare no competing interests.

Ethical Approval
Experimental protocol (No. 200A052022) was approved by the Institutional Animal Care and Use Committee (IACUC) of the Goldberg Research Institute of Pharmacology and Regenerative Medicine.

Funding
This work was supported by the Russian Science Foundation under Grant No. 24-15-00334.

Supplementary File
Supplementary file contains Table S1-S4.

References
1. Dunnington K, Benrimoh N, Brandquist C, Cardillo-Marrico N, Di Spirit M, Grenier J. Application of pharmacokinetics in early drug development. In: Malangu N, ed. Pharmacokinetics and Adverse Effects of Drugs - Mechanisms and Risks Factors. London, UK: IntechOpen; 2018. doi:10.5772/intechopen.74189
2. Andrade EL, Bento AF, Cavalli J, Oliveira SK, Schwanke RC, Siqueira JM, et al. Non-clinical studies in the process of new drug development-part II: good laboratory practice, metabolism, pharmacokinetics, safety and dose translation to clinical studies. Braz J Med Biol Res 2016;49(12): e5646. doi:10.1590/1414-431x20165646
3. Choi GW, Lee YB, Cho HY. Interpretation of non-clinical data for prediction of human pharmacokinetic parameters: in vitro-in vivo extrapolation and allometric scaling. Pharmaceutics 2019;11(4):168. doi:10.3390/pharmaceutics11040168
4. Duong MT, Lee JH, Ahn HC. C-Jun N-terminal kinase inhibitors: structural insight into kinase-inhibitor complexes. Comput Struct Biotechnol J 2020;18:1440-57. doi:10.1016/j.csbj.2020.06.013
5. Li G, Qi W, Li X, Zhao J, Luo M, Chen J. Recent advances in c-Jun N-terminal kinase (JNK) inhibitors. Curr Med Chem 2021;28(3):607-27. doi:10.2174/0929867327666200210144114
6. Wu Q, Wu W, Jacevic V, Franca TC, Wang X, Kuca K. Selective inhibitors for JNK signalling: a potential targeted therapy in cancer. J Enzyme Inhib Med Chem 2020;35(1):574-83. doi:10.1080/14756366.2020.1720013
7. Hepp Rehfeldt SC, Majolo F, Goettert MI, Laufer S. c-Jun N-terminal kinase inhibitors as potential leads for new therapeutics for Alzheimer's diseases. Int J Mol Sci 2020;21(24):9677. doi:10.3390/ijms21249677
8. Schepetkin IA, Khlebnikov AI, Potapov AS, Kovrizhina AR, Matveevskaya VV, Belyanin ML, et al. Synthesis, biological evaluation, and molecular modeling of 11H-indeno[1,2-b]quinoxalin-11-one derivatives and tryptanthrin-6-oxime as c-Jun N-terminal kinase inhibitors. Eur J Med Chem 2019;161:179-91. doi:10.1016/j.ejmech.2018.10.023
9. Plotnikov MB, Chernysheva GA, Smolyakova VI, Aliev OI, Trofimova ES, Sherstoboev EY, et al. Neuroprotective effects of a novel inhibitor of c-Jun N-terminal kinase in the rat model of transient focal cerebral ischemia. Cells 2020;9(8):1860. doi:10.3390/cells9081860
10. Plotnikov MB, Chernysheva GA, Aliev OI, Smol'yakova VA, Sidekhmenova AV, Dunaeva OI, et al. Effect of IQ-1 on the infarct size and the parameters of cardiodynamic indicators in the acute period after myocardial ischemia/reperfusion in rats. Bull Exp Biol Med 2024;176(4):447-51. doi:10.1007/s10517-024-06044-9
11. Schepetkin IA, Kirpotina LN, Hammaker D, Kochetkova I, Khlebnikov AI, Lyakhov SA, et al. Anti-inflammatory effects and joint protection in collagen-induced arthritis after treatment with IQ-1S, a selective c-Jun N-terminal kinase inhibitor. J Pharmacol Exp Ther 2015;353(3):505-16. doi:10.1124/jpet.114.220251
12. Seledtsov VI, Malashchenko VV, Meniailo ME, Atochin DN, Seledtsova GV, Schepetkin IA. Inhibitory effect of IQ-1S, a selective c-Jun N-terminal kinase (JNK) inhibitor, on phenotypical and cytokine-producing characteristics in human macrophages and T-cells. Eur J Pharmacol 2020;878:173116. doi:10.1016/j.ejphar.2020.173116
13. Plotnikov MB, Aliev OI, Shamanaev AY, Sidekhmenova AV, Anishchenko AM, Fomina TI, et al. Antihypertensive activity of a new c-Jun N-terminal kinase inhibitor in spontaneously hypertensive rats. Hypertens Res 2020;43(10):1068-78. doi:10.1038/s41440-020-0446-9
14. Atochin DN, Schepetkin IA, Khlebnikov AI, Seledtsov VI, Swanson H, Quinn MT, et al. A novel dual NO-donating oxime and c-Jun N-terminal kinase inhibitor protects against cerebral ischemia-reperfusion injury in mice. Neurosci Lett 2016;618:45-9. doi:10.1016/j.neulet.2016.02.033
15. Schepetkin IA, Kirpotina LN, Khlebnikov AI, Hanks TS, Kochetkova I, Pascual DW, et al. Identification and characterization of a novel class of c-Jun N-terminal kinase inhibitors. Mol Pharmacol 2012;81(6):832-45. doi:10.1124/mol.111.077446
16. Lakeev AP, Frelikh GA, Yanovskaya EA, Kovrizhina AR, Udut VV. Quantification of a promising JNK inhibitor and nitrovasodilator IQ-1 and its major metabolite in rat plasma by LC-MS/MS. Bioanalysis 2022;14(22):1423-41. doi:10.4155/bio-2022-0193
17. Yanovskaya EA, Frelikh GA, Lakeev AP, Chernysheva GA, Smol'yakova VI, Kovrizhina AR. Pharmacokinetics of a new neuroprotector - indenoquinoxalinone derivative after intravenous administration in rabbits and rats. Bull Exp Biol Med 2023;175(6):770-3. doi:10.1007/s10517-023-05943-7
18. Frelikh GA, Yanovskaya EA, Lakeev AP, Chernysheva GA, Smolyakova VI, Kovrizhina AR. Dose proportionality and bioavailability of quinoxaline-based JNK inhibitor after single oral and intravenous administration in rats. Xenobiotica 2024;54(1):18-25. doi:10.1080/00498254.2023.2299686
19. Obach RS. Pharmacologically active drug metabolites: impact on drug discovery and pharmacotherapy. Pharmacol Rev 2013;65(2):578-640. doi:10.1124/pr.111.005439
20. Cho S, Yoon YR. Understanding the pharmacokinetics of prodrug and metabolite. Transl Clin Pharmacol 2018;26(1):1-5. doi:10.12793/tcp.2018.26.1.1
21. Kirpotina LN, Schepetkin IA, Hammaker D, Kuhs A, Khlebnikov AI, Quinn MT. Therapeutic effects of tryptanthrin and tryptanthrin-6-oxime in models of rheumatoid arthritis. Front Pharmacol 2020;11:1145. doi:10.3389/fphar.2020.01145
22. European Parliament and the Council. Directive 2010/63/EU of the European Parliament and of the Council of 22 September 2010 on the Protection of Animals Used for Scientific Purposes Text with EEA Relevance. EUR-Lex; 2010. Available from: https://eur-lex.europa.eu/legal-content/EN/TXT/?uri=celex%3A32010L0063. Accessed September 22, 2023.
23. European Medicines Agency (EMA). Bioanalytical Method Validation - Scientific Guideline. EMA; 2015. Available from: https://www.ema.europa.eu/en/bioanalytical-method-validation-scientific-guideline. Accessed March 3, 2023.
24. Curry SH, Whelpton R. Drug Disposition and Pharmacokinetics: From Principles to Applications. 2nd ed. New Jersey: Wiley-

Blackwell; 2011.
25. Karlgren M, Bergström CA. How physicochemical properties of drugs affect their metabolism and clearance. In: Wilson AG, ed. New Horizons in Predictive Drug Metabolism and Pharmacokinetics. Cambridge: Royal Society of Chemistry; 2015. p. 1-26. doi:10.1039/9781782622376-00001
26. Lipinski CA. Lead- and drug-like compounds: the rule-of-five revolution. Drug Discov Today Technol 2004;1(4):337-41. doi:10.1016/j.ddtec.2004.11.007
27. Azman M, Sabri AH, Anjani QK, Mustaffa MF, Hamid KA. Intestinal absorption study: challenges and absorption enhancement strategies in improving oral drug delivery. Pharmaceuticals (Basel) 2022;15(8):975. doi:10.3390/ph15080975
28. Zhang N, Hua Y, Wang C, Sun Y, Wang Z, Liu Z, et al. Distribution study of tryptanthrin in rat tissues by HPLC and its relationship with meridian tropism of *Indigo naturalis* in traditional Chinese medicine. Biomed Chromatogr 2014;28(12):1701-6. doi:10.1002/bmc.3203
29. Li J, Miao S, Xie Y, Wang J, Cao W, Bi L, et al. Pharmacokinetics and tissue distribution study of tryptanthrin in rats by RP-HPLC with DAD detector. Chromatographia 2012;75(23):1415-20. doi:10.1007/s10337-012-2322-5
30. Zhang X, Xia J, Zhang W, Luo Y, Sun W, Zhou W. Study on pharmacokinetics and tissue distribution of single dose oral tryptanthrin in Kunming mice by validated reversed-phase high-performance liquid chromatography with ultraviolet detection. Integr Med Res 2017;6(3):269-79. doi:10.1016/j.imr.2017.05.001
31. Jähne EA, Eigenmann DE, Sampath C, Butterweck V, Culot M, Cecchelli R, et al. Pharmacokinetics and in vitro blood-brain barrier screening of the plant-derived alkaloid tryptanthrin. Planta Med 2016;82(11-12):1021-9. doi:10.1055/s-0042-105295
32. Plotnikov MB, Chernysheva GA, Smol'yakova VI, Aliev OI, Anishchenko AM, Ulyakhina OA, et al. Neuroprotective effects of tryptanthrin-6-oxime in a rat model of transient focal cerebral ischemia. Pharmaceuticals (Basel) 2023;16(8):1057. doi:10.3390/ph16081057
33. Brocks DR, Davies NM. Lymphatic drug absorption via the enterocytes: pharmacokinetic simulation, modeling, and considerations for optimal drug development. J Pharm Pharm Sci 2018;21(1s):254s-70s. doi:10.18433/jpps30217